

## Quantifying Possible Routes for SpnF-Catalyzed Formal Diels–Alder Cycloaddition

Michael G. Medvedev<sup>ab\*</sup>, Alexey A. Zeifman<sup>b</sup>, Fedor N. Novikov<sup>bc</sup>, Ivan S. Bushmarinov<sup>a\*</sup>, Oleg V. Stroganov<sup>bc</sup>, Ilya Yu. Titov<sup>bc</sup>, Ghermes G. Chilov<sup>bc\*</sup>, Igor V. Svitanko<sup>b</sup>

<sup>a</sup>X-ray Structural Laboratory, A.N. Nesmeyanov Institute of Organoelement Compounds RAS, 119991 Moscow, Russian Federation

<sup>b</sup>N.D. Zelinsky Institute of Organic Chemistry RAS, 119991 Moscow, Russian Federation

<sup>c</sup>MolTech Ltd., Leninskie gory, 1/75 A, 119992 Moscow, Russian Federation

Computational details.....	2
Search for [4+2] transition states .....	2
Search for additional Diels-Alder (DA) and bis-pericyclic (BPC) transition states .....	3
Search for reagents' structures for DA and BPC mechanisms .....	4
Search for products' structures for DA and BPC mechanisms.....	4
Search for additional TSs' and target products' structures for the BPC mechanism .....	5
Search for biradical transition states.....	6
Search for "alternative Diels-Alder" (altDA) transition states .....	7
Search for reagents' structures for the altDA mechanism .....	7
Search for additional TSs', intermediates' and products' structures for the altDA mechanism .....	8
Recomputation of important stationary points' energies with PBE0-D3 .....	10
Cartesian coordinates and energies of located stationary points .....	11
QTAIM analysis .....	12
C2–C14 atoms connectivity .....	12
Calculation of contributions to the reaction flow using the Curtin-Hammett principle.....	13
Figure S1. Notched box plots of thermally uncorrected energies from M06-2X and PBE0-D3 calculations. ....	14
Figure S2. Overview of located conformations of DA and PBC transition states.....	15
Figure S3. Comparison of relative energies of DA and BPC TSs having a given bond path to the overall distribution. ....	16
Figure S4. Structures of the lowest-energy transition states of DA and BPC mechanisms.....	17
Figure S5. Relative energies of DA and BPC TSs vs. selected interatomic distances.....	18
Figure S6. Simplified scheme of stationary points searches and analyses performed in this study.....	19
Figure S7. Example geometries of located [4+2] transition states. ....	20
Figure S8. Comparison between common BPC and BR-1T transition states. ....	21
Figure S9. Examples of located altDA transition states. ....	22
References .....	23

## Computational details

A simplified scheme of stationary points search and analysis workflow performed in this study is introduced on Figure S6. All quantum chemical calculations were performed with Gaussian09 D.01<sup>1</sup>.

### Search for [4+2] transition states

On the first step, we have generated all possible conformers of the product **P**. This was done using the recently developed method<sup>2</sup> dedicated especially for macrocycles. It appeared to be effective for **P**: four separate executions, starting from significantly different initial structures resulted in almost identical sets of ~500 structures each. All 1971 generated structures were combined and optimized by MM3 molecular mechanics method to the closest minima. Duplicates with root mean square deviation of non-hydrogen atom coordinates (further  $\text{RMSD}_{\text{non-hydrogen}}$ ) below 0.2 Å were removed to leave 560 unique conformers of **P**. Notably, the fourth run of the conformer generator contributed only 16 unique conformers.

After that the following procedure was applied to each conformer:

1. Bonds C7–C11 and C4–C12 were constrained to be 1.95 Å and 2.6 Å, respectively (these values were taken from several preliminary located TSs), while distance C2–C14 was fixed at its initial length to avoid formation of a new bond. Unconstrained internal coordinates were relaxed to minimize the energy at B97D<sup>3</sup>/3-21G\*<sup>4</sup> grid=sg1 level of theory.
2. Constraints were relaxed and search for the closest transition state (TS) was performed at M06-2X<sup>5</sup>/6-31+G(d)<sup>6</sup> grid=ultrafine level of theory with implicit water modeled with PCM. This level of theory was shown<sup>7,8</sup> to provide energies and geometries close to those from the CCSD<sup>9</sup> method for TSs of different Diels-Alder reactions.
3. Harmonic frequencies were calculated at the same level of theory as in the previous step to ascertain that found stationary point is TS. Imaginary frequency's normal mode direction was checked. Zero-point energies and thermal corrections at 298.15 K calculated at this stage were used later in the analysis of the mechanisms' interplay.

This approach led to 429 [4+2] TSs with energies relative to the lowest conformation ( $E_{\text{rel}}$ ) less than 30 kcal/mol. Examination of the remaining 131 cases showed that their initial product geometries are too twisted to be directly formed by Diels-Alder cyclization (see Fig. S6); they also have very high relative energies. Found TSs were purified from duplicates ( $\text{RMSD}_{\text{non-hydrogen}} < 0.2$  Å) to yield a total of 376 unique transition states. All of them have very similar geometries of the reacting part (Figure S2) differing by the synchronicity of the cycloaddition.

These 376 TSs represent all possible conformations convenient for formation of **P** via C4–C12 and C7–C11 bonds closure, so we used their geometries in searches for TSs of other routes.

Search for additional Diels-Alder (DA) and bis-pericyclic (BPC) transition states

Transition states generated on the previous stage may belong to either **DA** or **BPC** mechanisms. However, there could be some additional **BPC** or [6+4] TSs, which differ from already located **DA** TSs by decreased C2–C14 distance and, probably, increased C4–C12 distance. A search for them starting from all 376 previously found structures was carried out using the following procedure:

1. Distances C2–C14 and C4–C12 were increased by 0.5 Å and fixed together with C7–C11 distance. Unconstrained internal coordinates were relaxed to minimize the energy at B97D/3-21G\* grid=sg1 level of theory.
2. Distances C2–C14, C4–C12 and C7–C11 were constrained to 2.6 Å, 3.6 Å, and 1.9 Å, respectively. Unconstrained internal coordinates were relaxed to minimize the energy at B97D/3-21G\* grid=sg1 level of theory.
3. Constraints were relaxed and search for the closest transition state (TS) was performed at M06-2X/6-31+G(d) grid=ultrafine level of theory with implicit water modeled with PCM.
4. Harmonic frequencies were calculated at the same level of theory as in the previous step to ascertain that found stationary point is TS. Imaginary frequency's normal mode direction was checked.

This search resulted in 8 additional unique TSs. Notably, *this search was designed to find [6+4] transition states*, but all 8 new TSs are **BPC**, as revealed by further QTAIM study.

For all already found TSs with C2–C14 shorter than  $(\text{length}(\text{C4–C12}) + 0.1 \text{ \AA})$  an additional search for TSs with increased C2–C14 distance was also performed using the following procedure:

1. Distance C2–C14 was enlarged by 0.5 Å and distance C4–C12 was shortened by 0.1 Å. An unconstrained search for the closest transition state (TS) was performed at M06-2X/6-31+G(d) grid=ultrafine level of theory with implicit water modeled with PCM.
2. Harmonic frequencies were calculated at the same level of theory as in the previous step to ascertain that found stationary point is TS. Imaginary frequency's normal mode direction was checked.

No new TSs were found.

#### Search for reagents' structures for DA and BPC mechanisms

Search for **S** was performed by applying the following procedure to each of 384 located TS:

1. Distances C2–C14, C4–C12 and C7–C11 were enlarged by 0.3 Å and fixed. Unconstrained internal coordinates were relaxed to minimize the energy at B97D/3-21G\* grid=sg1 level of theory.
2. Constraints were relaxed and search for the closest minimum was performed at B97D/3-21G\* grid=sg1 level of theory.
3. Using obtained geometry, an unconstrained search for the closest minimum was performed at M06-2X/6-31+G(d) grid=ultrafine level of theory with implicit water modeled with PCM.
4. Harmonic frequencies were calculated at the same level of theory as in the previous step to ascertain that found stationary point is minimum.

384 structures of **S** were obtained.

#### Search for products' structures for DA and BPC mechanisms

Search for products connected with located TSs was performed by applying the following procedure to each found TS:

1. The intrinsic reaction coordinate was followed in the direction of product for 10 steps at M06-2X/6-31+G(d) grid=ultrafine level of theory with implicit water modeled with PCM.
2. Then a search for the closest minimum was performed at B97D/3-21G\* grid=sg1 level of theory.
3. Using obtained geometry, a search for the closest minimum was performed at M06-2X/6-31+G(d) grid=ultrafine level of theory with implicit water modeled with PCM.
4. Harmonic frequencies were calculated at the same level of theory as in the previous step to ascertain that found stationary point is minimum.

371 of obtained structures correspond to **P** and the rest 13 correspond to **I-[6+4]**.

Search for additional TSs' and target products' structures for the BPC mechanism

For each of 13 located **I-[6+4]**, a search for **Cope** TS was performed as follows:

1. Distances C2–C14, C4–C12 and C7–C11 were constrained to 2.3 Å, 2.3 Å, and 1.6 Å, respectively (these values were taken from several preliminary located TSs). Unconstrained internal coordinates were relaxed to minimize the energy at B97D/3-21G\* grid=sg1 level of theory.
2. A search for closest transition state was performed at M06-2X/6-31+G(d) grid=ultrafine level of theory with implicit water modeled with PCM.
3. Harmonic frequencies were calculated at the same level of theory as in the previous step to ascertain that found stationary point is TS. Imaginary frequency's normal mode direction was checked.

A search for the corresponding products **P** was performed starting from **I-[6+4]** as follows:

1. Distances C4–C12 and C7–C11 were constrained to 1.58 Å and 1.56 Å, respectively. Unconstrained internal coordinates were relaxed to minimize the energy at B97D/3-21G\* grid=sg1 level of theory.
2. A search for closest minimum was performed at M06-2X/6-31+G(d) grid=ultrafine level of theory with implicit water modeled with PCM.
3. Harmonic frequencies were calculated at the same level of theory as in the previous step to ascertain that found stationary point is minimum.

These searches have located 13 **Cope** TSs and 13 **P**.

### Search for biradical transition states

Search for triplet biradical TSs **BR-1T** was performed by applying the following procedure to each of 376 conformers generated on the first stage:

1. Distance C7–C11 was increased to 1.96 Å and an unconstrained search for the closest triplet transition state was performed at broken-symmetry uBHandHLYP<sup>10</sup>/6-31+G(d) level of theory with implicit water modeled with PCM.
2. Using the obtained geometry, a search for the closest transition state (TS) was performed at broken-symmetry uM06-2X/6-31+G(d) grid=ultrafine level of theory with implicit water modeled with PCM. M06-2X is known to produce suitable energies and geometries for organic biradical species<sup>11</sup>.  
Wavefunction was checked for instabilities by Gaussian “stable” routine to ascertain its stability.
3. Harmonic frequencies were calculated at the same level of theory as in the previous step to ascertain that found stationary point is TS. Imaginary frequency’s normal mode direction was checked.

This produced 356 triplet **BR-1T** TSs. For the rest 20 cases triplet TSs could not be located even by varying the C7–C11 bond length in the first step of our procedure. Found **BR-1T** TSs were purified from duplicates ( $\text{RMSD}_{\text{non-hydrogen}} < 0.2 \text{ \AA}$ ) to yield a total of 331 unique triplet transition states. Structures of common **BPC** and **BR-1T** transition states (the **BR-1T** is obtained directly from that **BPC**) are shown in Figure S8.

After that, a search for singlet biradical TSs **BR-1S** was performed by applying the following procedure to each of 331 unique conformations of **BR-1T**:

1. A search for the closest singlet biradical transition state (TS) was performed at broken-symmetry uM06-2X/6-31+G(d) grid=ultrafine guess=(INDO, mix) level of theory with implicit water modeled with PCM.  
Wavefunction was checked for instabilities by Gaussian “stable” routine to ascertain its stability.
2. Harmonic frequencies were calculated at the same level of theory as in the previous step to ascertain that found stationary point is TS. Imaginary frequency’s normal mode direction was checked.

Only 9 singlet biradical TSs were located, while all other calculations converged to either non-biradical singlet TSs (**DA** or **BPC**) or to non-biradical TSs between two substrates’ conformations.

#### Search for “alternative Diels-Alder” (altDA) transition states

Finally, search for **altDA** transition states was performed by applying the following procedure to each of 376 conformers generated on the first stage:

1. Distances C2–C14 and C5–C13 were changed stepwise (to avoid calculation failure) to 2.5 Å each, and C7–C11 distance was increased by 0.5 Å. These three distances were fixed. Unconstrained internal coordinates were relaxed to minimize the energy at B97D/3-21G\* grid=sg1 level of theory.
2. Constraints were relaxed and search for the closest transition state was performed at B97D/6-31+G(d) level of theory with implicit water modeled with PCM.
3. A search for closest transition state was performed at M06-2X/6-31+G(d) grid=ultrafine level of theory with implicit water modeled with PCM.
4. Harmonic frequencies were calculated at the same level of theory as in the previous step to ascertain that found stationary point is TS. Imaginary frequency’s normal mode direction was checked.

This search found 4 transition states belonging to **altDA** mechanism. Structures of two of them are shown in Figure S9.

#### Search for reagents’ structures for the altDA mechanism

Search for **S** was performed by applying the following procedure to each **altDA** TS:

1. Distances C2–C14, C5–C13 and C7–C11 were enlarged by 0.3 Å and fixed. Unconstrained internal coordinates were relaxed to minimize the energy at B97D/3-21G\* grid=sg1 level of theory.
2. Constraints were relaxed and search for the closest minimum was performed at M06-2X/6-31+G(d) grid=ultrafine level of theory with implicit water modeled with PCM.
3. Harmonic frequencies were calculated at the same level of theory as in the previous step to ascertain that found stationary point is minimum.

4 structures of **S** were obtained.

Search for additional TSs', intermediates' and products' structures for the **altDA** mechanism

Search for **I-altDA** intermediates, connected with located **altDA** TSs was performed by applying the following procedure to each found TS:

1. Distances C2–C14 and C5–C13 were constrained to 1.6 Å each. Unconstrained internal coordinates were relaxed to minimize the energy at B97D/3-21G\* grid=sg1 level of theory.
2. A search for closest minimum was performed at M06-2X/6-31+G(d) grid=ultrafine level of theory with implicit water modeled with PCM.
3. Harmonic frequencies were calculated at the same level of theory as in the previous step to ascertain that found stationary point is minimum.

4 structures of **I-altDA** were obtained.

For each of 4 **I-altDA** located, a search for **altCope** TS was performed as follows:

1. Distances C2–C14, C5–C13 and C7–C11 were constrained to 1.6, 2.3 and 2.3 Å, respectively. Unconstrained internal coordinates were relaxed to minimize the energy at B97D/3-21G\* grid=sg1 level of theory.
2. A search for closest transition state was performed at M06-2X/6-31+G(d) grid=ultrafine level of theory with implicit water modeled with PCM.
3. Harmonic frequencies were calculated at the same level of theory as in the previous step to ascertain that found stationary point is TS. Imaginary frequency's normal mode direction was checked.

A search for the corresponding products **I-[6+4]** was performed starting from **altCope** structures as follows:

1. Distances C2–C14 and C7–C11 were constrained to 1.58 Å and 1.56 Å, respectively. Unconstrained internal coordinates were relaxed to minimize the energy at B97D/3-21G\* grid=sg1 level of theory.
2. A search for closest minimum was performed at M06-2X/6-31+G(d) grid=ultrafine level of theory with implicit water modeled with PCM.
3. Harmonic frequencies were calculated at the same level of theory as in the previous step to ascertain that found stationary point is minimum.

A search for the corresponding **Cope** TSs was performed starting from **I-[6+4]** structures as follows:

1. Distances C2–C14, C4–C12 and C7–C11 were constrained to 2.3 Å, 2.3 Å, and 1.6 Å, respectively. Unconstrained internal coordinates were relaxed to minimize the energy at B97D/3-21G\* grid=sg1 level of theory.
2. A search for closest transition state was performed at M06-2X/6-31+G(d) grid=ultrafine level of theory with implicit water modeled with PCM.
3. Harmonic frequencies were calculated at the same level of theory as in the previous step to ascertain that found stationary point is TS. Imaginary frequency's normal mode direction was checked.

A search for the corresponding products **P** was performed starting from **Cope** structures as follows:

1. Distances C4–C12 and C7–C11 were constrained to 1.58 Å and 1.56 Å, respectively. Unconstrained internal coordinates were relaxed to minimize the energy at B97D/3-21G\* grid=sg1 level of theory.
2. A search for closest minimum was performed at M06-2X/6-31+G(d) grid=ultrafine level of theory with implicit water modeled with PCM.
3. Harmonic frequencies were calculated at the same level of theory as in the previous step to ascertain that found stationary point is minimum.

These searches have found 4 structures of each type: **altCope**, **Cope**, **I-altDA**, **I-[6+4]** and **P**.

### Recomputation of important stationary points' energies with PBE0-D3

Single-point energies of all **S**, **DA**, **BPC**, **BR-1S**, **BR-1T** and **altDA** structures located with M06-2X were computed at PBE0-D3/6-31+G(d) grid=ultrafine level of theory with implicit water modeled with PCM. Relative energies of **DA** and **BPC** TSs were found to be qualitatively identical:

$$E_{M06-2X} = -1.0 + 0.95 * E_{PBE0-D3} \quad ; \quad R^2 = 97\%$$

This is likely caused by a favorable error cancellation arising from the fact that all **DA** and **BPC** TSs are similar in nature, so the functionals' systematic errors largely cancel out<sup>12</sup>.

According to PBE0-D3 data, the **BPC** path is responsible for 92% of the reaction flow (thermal corrections are not included, because calculations are carried on non-optimized geometries). At PBE0-D3 level of theory, the lowest **BR-1S** and **BR-1T** TSs lie 12 and 21 kcal mol<sup>-1</sup> above the lowest singlet TS, respectively, and the lowest **altDA** TS lies 38 kcal mol<sup>-1</sup> above it. All conclusions of the paper remain unchanged in the light of the PBE0-D3 data.

## Cartesian coordinates and energies of located stationary points

Cartesian coordinates of all located stationary points are available as a set of xyz files:

- Non-BR\_TS.xyz contains 388 structures of located non-biradical transition states: **DA**, **BPC** and **altDA**. Structures 1, 2, 4, 5, 6, 8, 9, 11, 14, 15, 17, 18, 19, 23, 25, 26, 27, 28, 29, 31, 32, 33, 36, 37, 38, 41, 42, 43, 45, 46, 47, 48, 51, 52, 53, 55, 56, 57, 59, 60, 61, 62, 67, 68, 70, 73, 75, 76, 77, 78, 80, 81, 82, 83, 87, 88, 90, 92, 94, 95, 97, 98, 99, 101, 102, 104, 105, 106, 107, 108, 109, 112, 113, 117, 119, 122, 123, 124, 125, 130, 131, 134, 135, 136, 137, 139, 140, 141, 142, 143, 144, 145, 147, 148, 150, 151, 152, 153, 154, 155, 156, 158, 160, 163, 167, 169, 176, 177, 179, 180, 181, 182, 183, 186, 187, 188, 189, 190, 191, 192, 193, 194, 196, 197, 200, 201, 202, 203, 204, 205, 206, 209, 210, 211, 214, 216, 219, 221, 222, 223, 224, 225, 226, 230, 234, 236, 238, 239, 240, 241, 242, 244, 245, 247, 248, 249, 252, 254, 255, 257, 258, 259, 260, 262, 263, 264, 265, 267, 268, 269, 270, 271, 273, 274, 275, 276, 277, 279, 281, 282, 283, 284, 285, 286, 287, 288, 289, 292, 293, 298, 299, 301, 304, 305, 307, 310, 311, 312, 313, 314, 315, 316, 319, 320, 321, 322, 323, 326, 330, 331, 334, 335, 336, 340, 342, 343, 344, 345, 346, 349, 350, 351, 353, 355, 356, 357, 358, 359, 360, 361, 362, 364, 365, 366, 367, 369, 370, 371, 372, 373 correspond to **DA** TSs. Structures 0, 3, 7, 10, 12, 13, 16, 20, 21, 22, 24, 30, 34, 35, 39, 40, 44, 49, 50, 54, 58, 63, 64, 65, 66, 69, 71, 72, 74, 79, 84, 85, 86, 89, 91, 93, 96, 100, 103, 110, 111, 114, 115, 116, 118, 120, 121, 126, 127, 128, 129, 132, 133, 138, 146, 149, 157, 159, 161, 162, 164, 165, 166, 168, 170, 171, 172, 173, 174, 175, 178, 184, 185, 195, 198, 199, 207, 208, 212, 213, 215, 217, 218, 220, 227, 228, 229, 231, 232, 233, 235, 237, 243, 246, 250, 251, 253, 256, 261, 266, 272, 278, 280, 290, 291, 294, 295, 296, 297, 300, 302, 303, 306, 308, 309, 317, 318, 324, 325, 327, 328, 329, 332, 333, 337, 338, 339, 341, 347, 348, 352, 354, 363, 368, 374, 375, 376, 377, 378, 379, 380, 381, 382, 383 correspond to **BPC** TSs. Structures 384, 385, 386, 387 correspond to **altDA** TSs.
- BR-1S.xyz contains 9 structures of located singlet biradical transition states – **BR-1S**.
- BR-1T.xyz contains 331 structures of located triplet biradical transition states – **BR-1T**.
- S.xyz contains 388 structures of located substrate conformers – **S**. Sequential number of **S** in the file correspond to the sequential number of TS it was obtained from.
- P.xyz contains 388 structures of located product conformers – **P**. Sequential number of **P** in the file correspond to the sequential number of TS it was obtained from.

Energies of all located stationary points (both thermally-corrected (M06-2X) and uncorrected (M06-2X and PBE0-D3)) are provided in Energies.xlsx supplementary file. All energies are in kcal mol<sup>-1</sup>.

## QTAIM analysis

Connectivity in located stationary points was studied in terms of QTAIM<sup>13,14</sup> using the AIMAll package<sup>15</sup> (version 16.08.17). All calculations were performed with default settings. M06-2X electron densities computed at M06-2X geometries were used for QTAIM calculations.

### C2–C14 atoms connectivity

Atoms C2 and C14 were considered bonded if a QTAIM bond path was found between them or between one of them and one of the three atoms, covalently bonded to the second. This was done because the use of a finite basis set and an approximate density functional can lead to deviations in density leading to errors in bond path connectivity.

Basing on C2–C14 connectivity, TSs were classified as **DA** or **BPC**. The lowest-energy structures of each type and their connectivities are shown in Figure S4.

## Calculation of contributions to the reaction flow using the Curtin-Hammett principle

Curtin-Hammett principle in its modern sense states, that the rate (and so, the efficacy) of a particular reaction path is determined by relative energies of the corresponding TSs, assuming that the rate of interconversion between substrate conformers is much higher than that of a chemical reaction<sup>16</sup>. Namely, for any two different transition states with energies  $E_1$  and  $E_2$ , their contributions to the reaction ( $C_1$  and  $C_2$ ) are connected as following:

$$\frac{C_1}{C_2} = \exp\left(\frac{E_2 - E_1}{R \times T}\right)$$

where  $R$  is the gas constant and  $T$  is the temperature.

This equation was used to calculate contribution ratios between each TS and the lowest one, and then individual percentage contributions were calculated by considering the cumulative contribution to be 100%.

Thermally-corrected (including zero-point correction, as well as vibrational, rotational, translational, enthalpy and entropy corrections at 298 K) energies of transition states were used to calculate contributions of each TS to the reaction. Use of uncorrected energies also resulted in the same contributions of **DA** and **BPC** routes (17% and 83%, respectively), but contributions of individual TSs were slightly different.

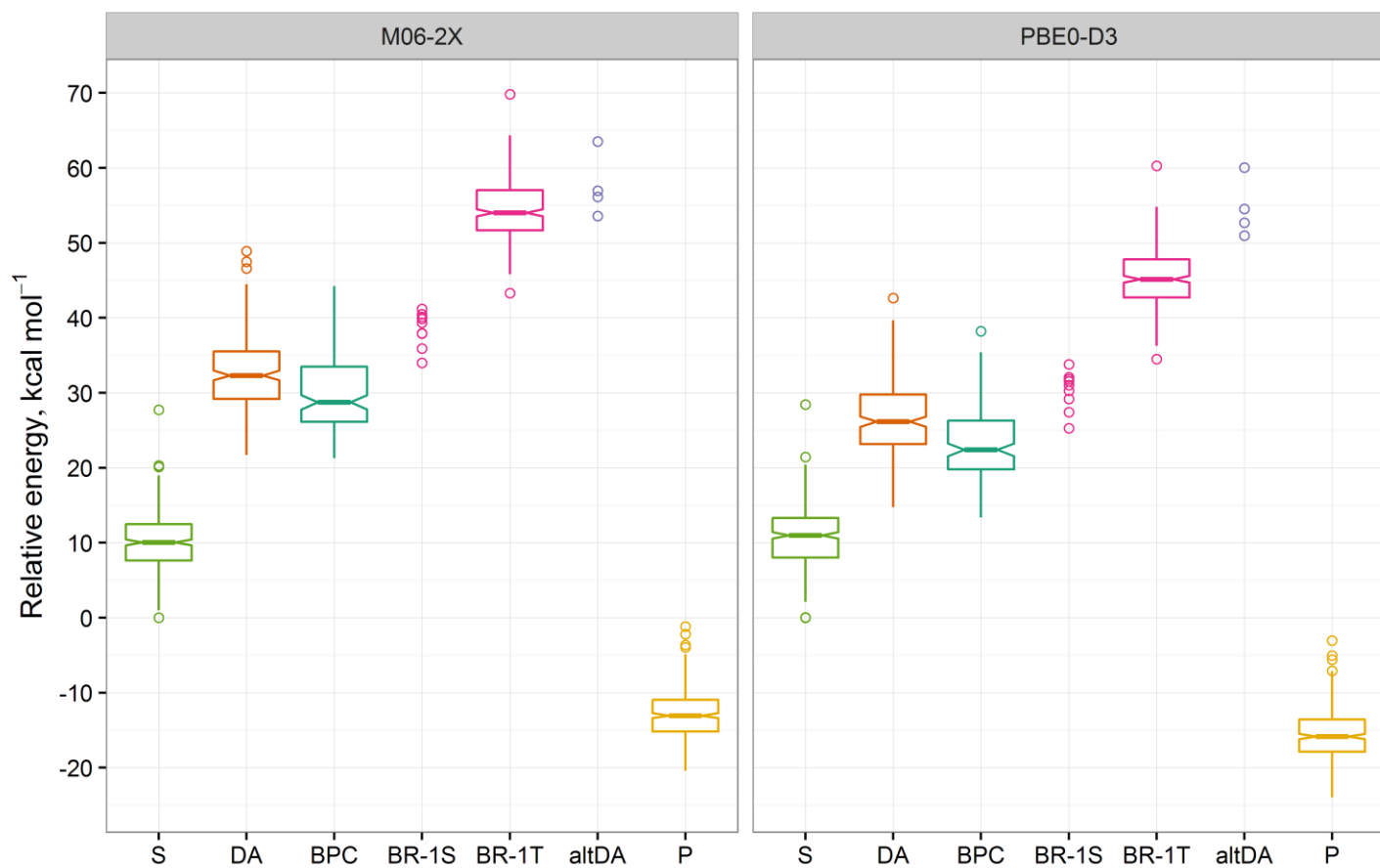


Figure S1. Notched box plots of thermally uncorrected energies from M06-2X and PBE0-D3 calculations.

Notches denote 95% confidence intervals of medians.

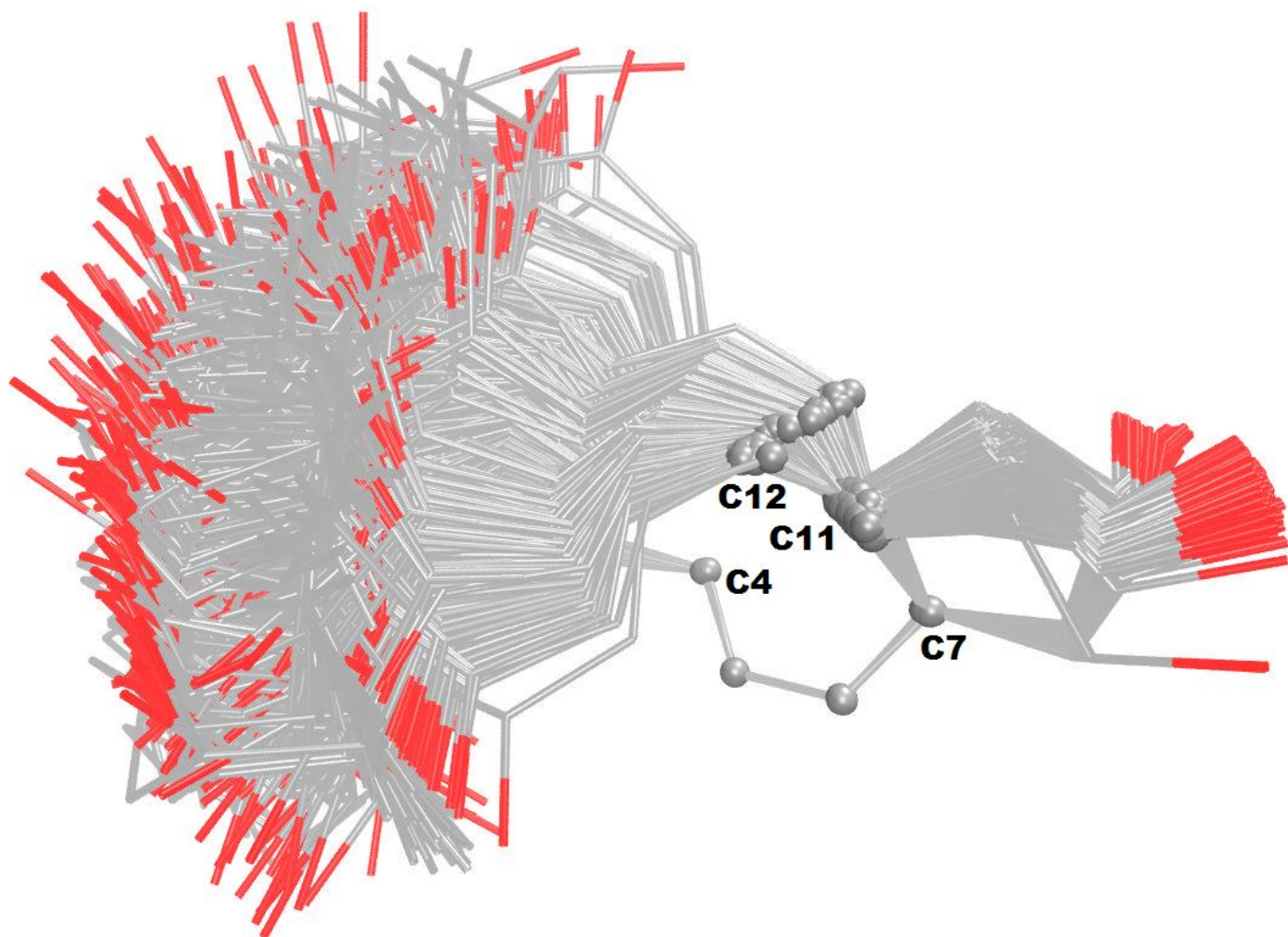


Figure S2. Overview of located conformations of DA and PBC transition states. Conformations are aligned by C4–C7–C11–C12 fragments, hydrogen atoms are omitted for clarity.

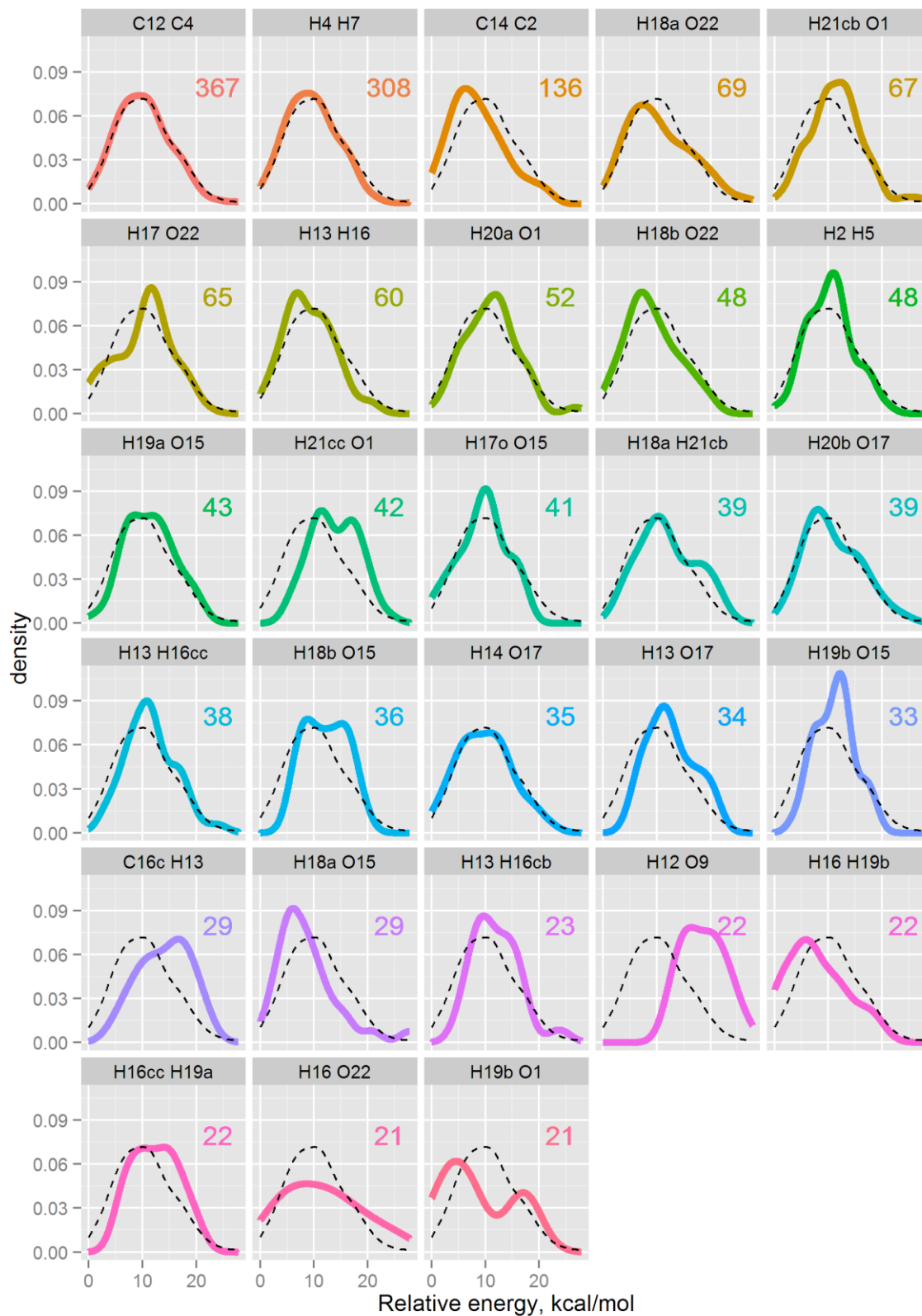


Figure S3. Comparison of relative energies of DA and BPC TSs having a given bond path to the overall distribution.

Count of structures with such bond path is denoted by a number on the subplot.

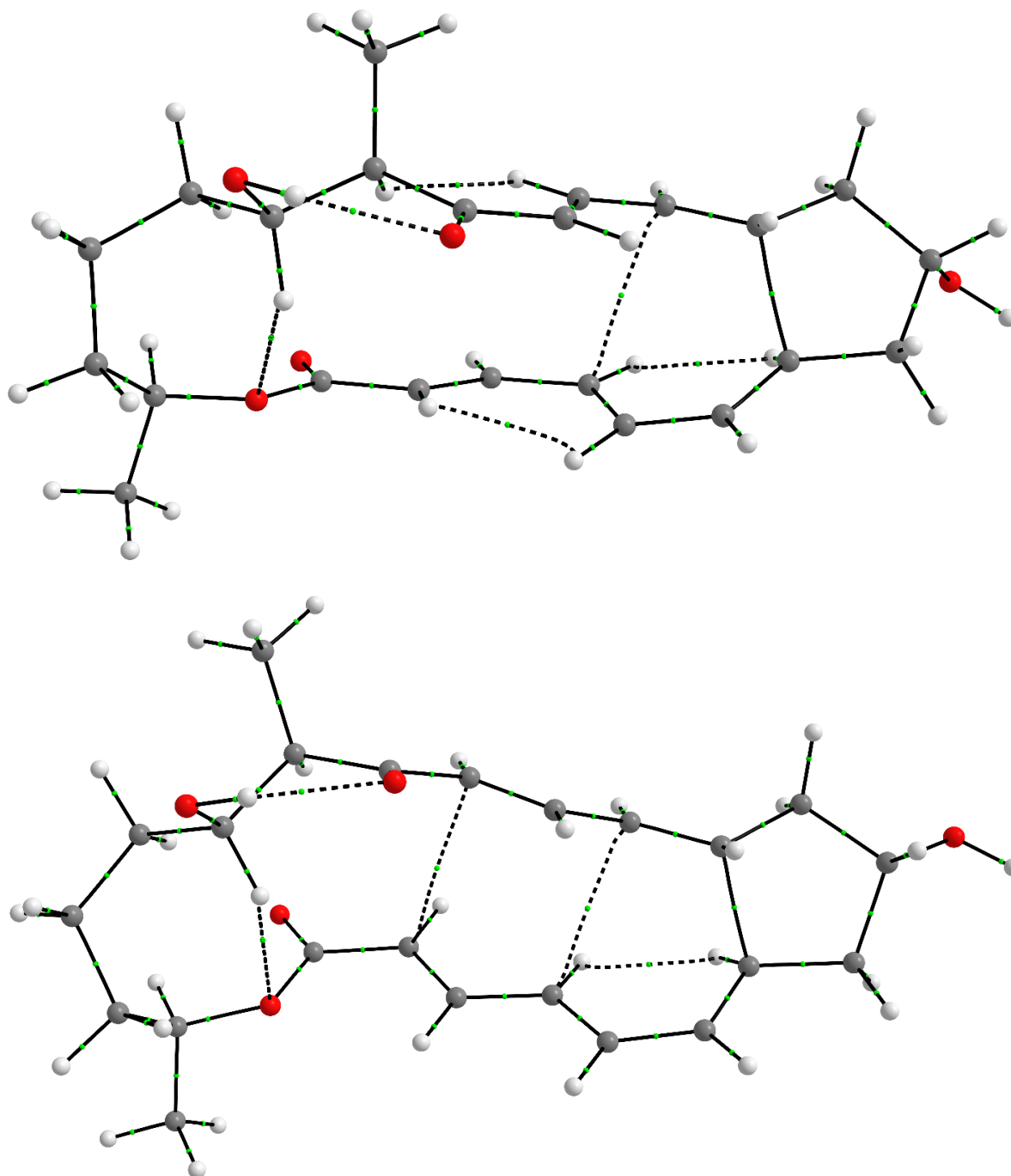


Figure S4. Structures of the lowest-energy transition states of DA and BPC mechanisms.

Top (TS #197) corresponds to **DA** and bottom (TS #120) corresponds to **BPC** mechanisms. Critical points (3, -1) from the QTAIM analysis are denoted by green dots (those with local electron density  $< 0.01$ , as well as all (3, +1) and (3, +3) ones, are omitted for clarity).

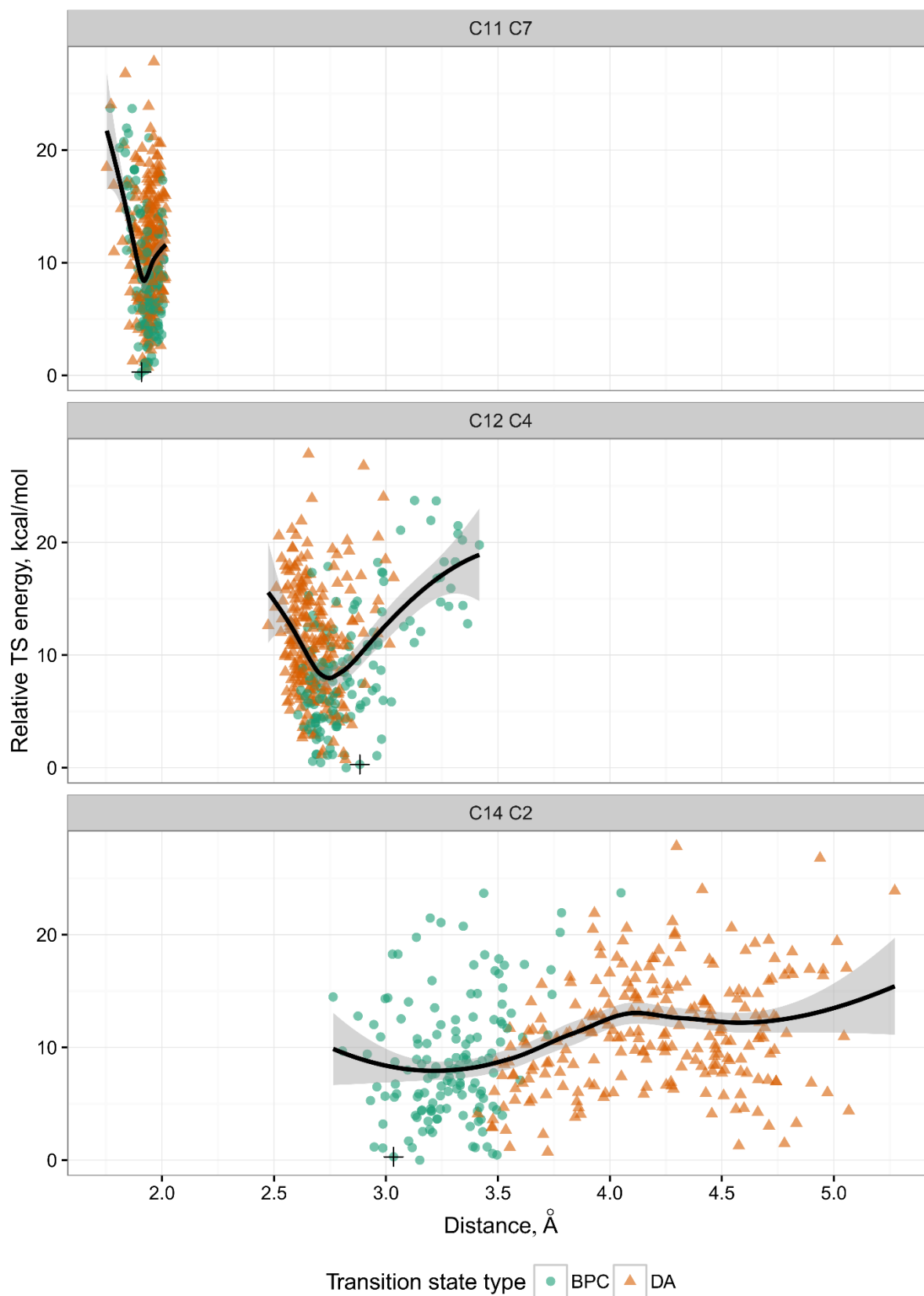


Figure S5. Relative energies of DA and BPC TSs vs. selected interatomic distances.

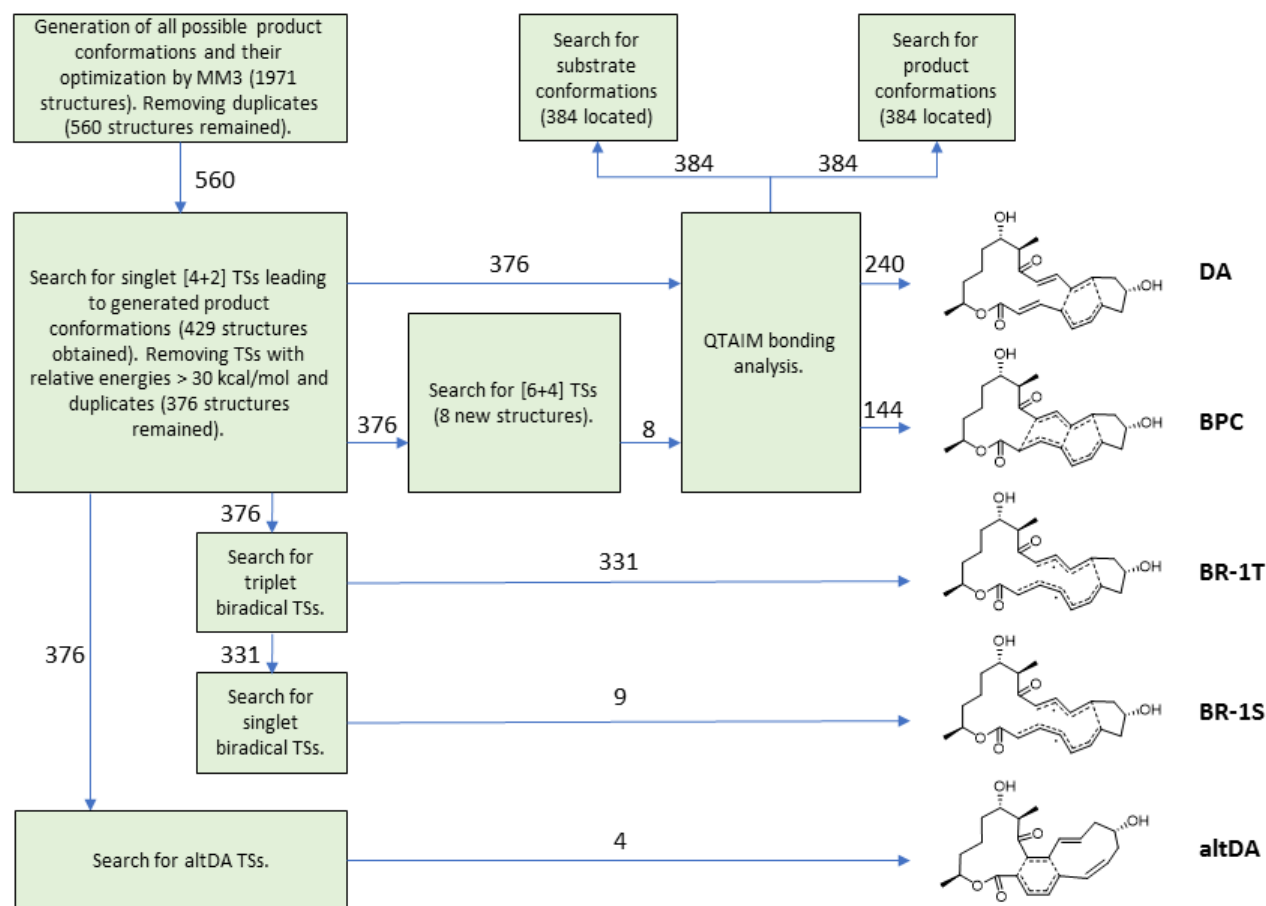
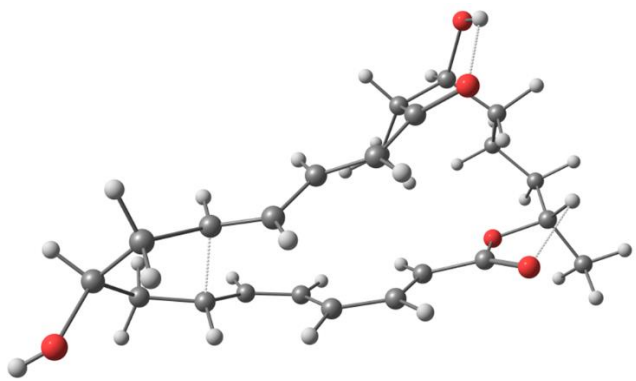
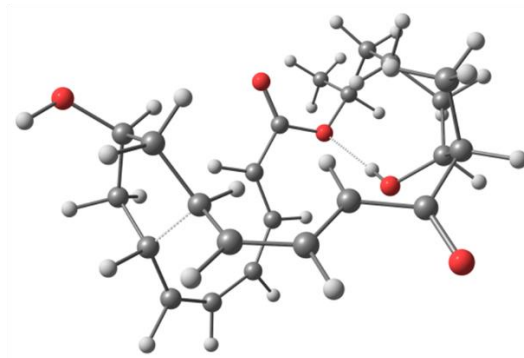


Figure S6. Simplified scheme of stationary points searches and analyses performed in this study.



$E_{rel} = 7.5$  kcal/mol



$E_{rel} = 51.3$  kcal/mol

Figure S7. Example geometries of located [4+2] transition states.

The left conformation belongs to normal ones and the right leads to a product that is too twisted to be directly formed by Diels-Alder cyclization.

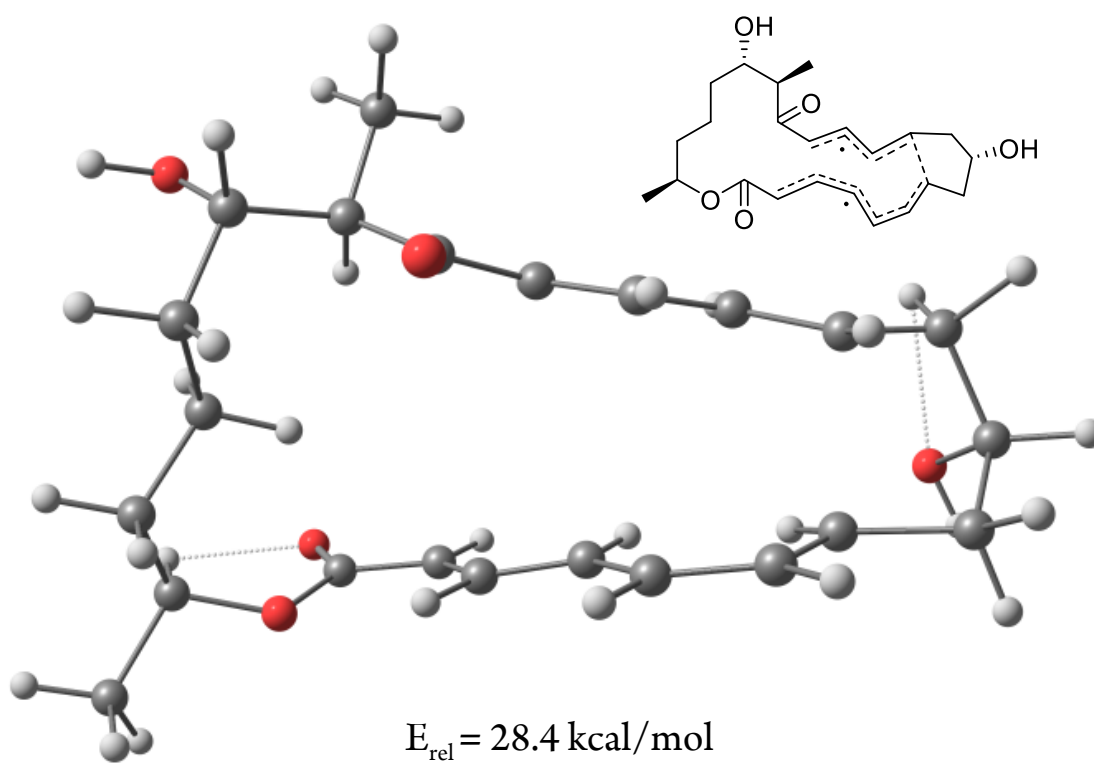
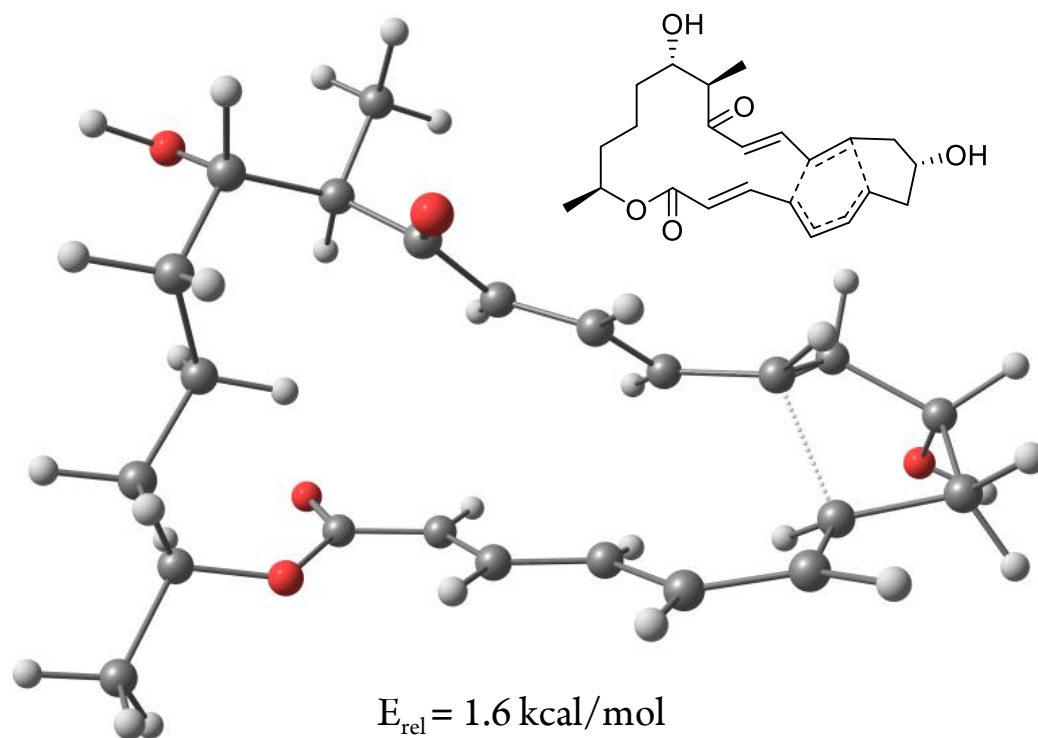


Figure S8. Comparison between common BPC and BR-1T transition states.

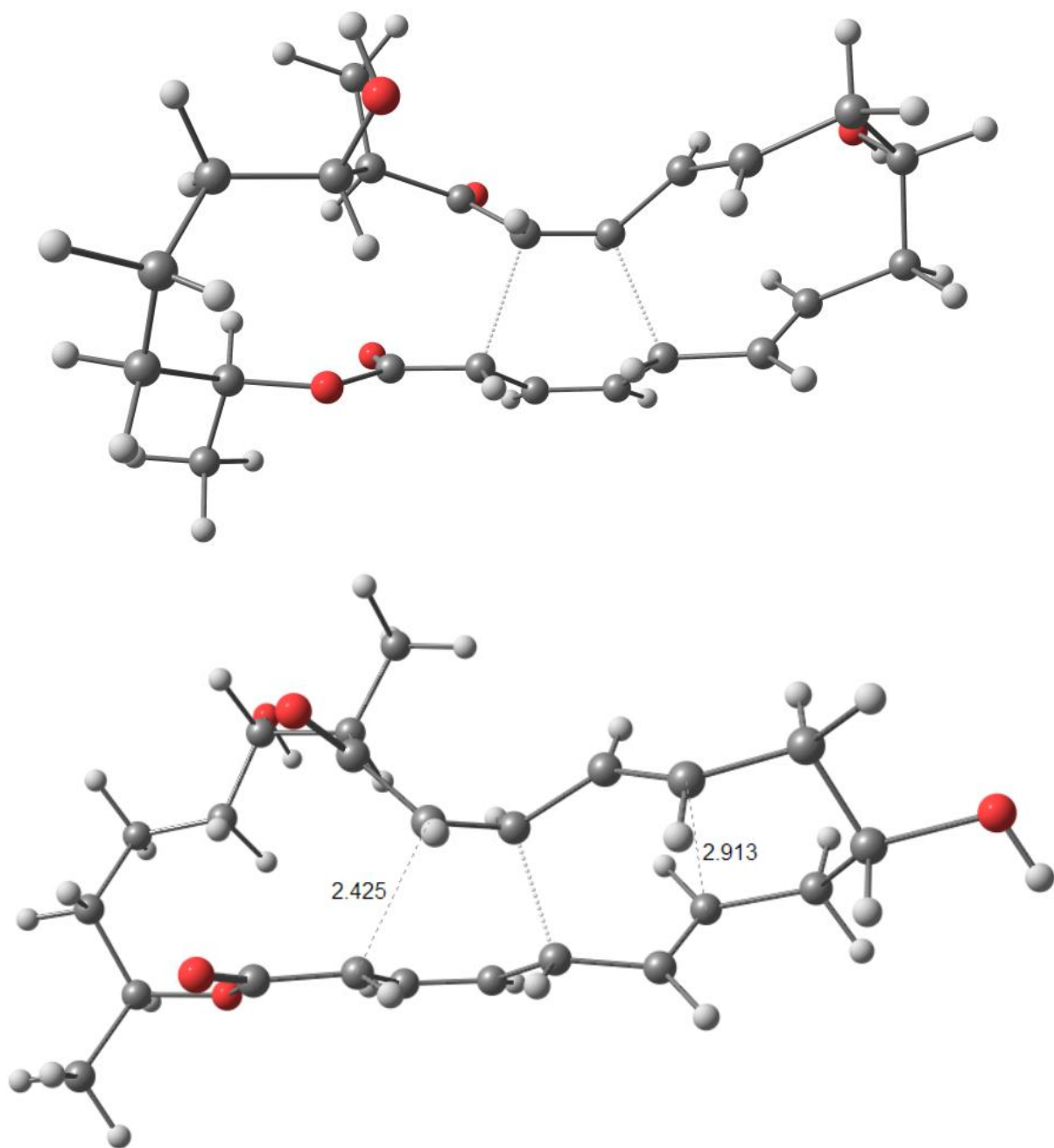


Figure S9. Examples of located *altDA* transition states.

## References

- (1) Frisch, M. J.; Trucks, G. W.; Schlegel, H. B.; Scuseria, G. E.; Robb, M. A.; Cheeseman, J. R.; Scalmani, G.; Barone, V.; Mennucci, B.; Petersson, G. A.; et al. *Gaussian 09, Revision D.01*.
- (2) Bonnet, P.; Agrafiotis, D. K.; Zhu, F.; Martin, E. *J. Chem. Inf. Model.* **2009**, *49*, 2242–2259.
- (3) Becke, A. D. *J. Chem. Phys.* **1997**, *107*, 8554.
- (4) Pietro, W. J.; Francl, M. M.; Hehre, W. J.; DeFrees, D. J.; Pople, J. A.; Binkley, J. S. *J. Am. Chem. Soc.* **1982**, *104*, 5039–5048.
- (5) Zhao, Y.; Truhlar, D. G. *Theor. Chem. Acc.* **2007**, *120*, 215–241.
- (6) Hehre, W. J.; Ditchfield, R.; Pople, J. A. *J. Chem. Phys.* **1972**, *56*, 2257–2261.
- (7) Linder, M.; Brinck, T. *Phys. Chem. Chem. Phys.* **2013**, *15*, 5108–5114.
- (8) Peverati, R.; Truhlar, D. G. *Philos. Trans. R. Soc. Lond. Math. Phys. Eng. Sci.* **2014**, *372*, 20120476.
- (9) Scuseria, G. E.; Janssen, C. L.; Schaefer III, H. F. *J. Chem. Phys.* **1988**, *89*, 7382–7387.
- (10) Becke, A. D. *J. Chem. Phys.* **1993**, *98*, 1372–1377.
- (11) Thomas, A.; Krishna Chaitanya, G.; Bhanuprakash, K.; Krishna Prasad, K. M. M. *ChemPhysChem* **2011**, *12*, 3458–3466.
- (12) Medford, A. J.; Wellendorff, J.; Vojvodic, A.; Studt, F.; Abild-Pedersen, F.; Jacobsen, K. W.; Bligaard, T.; Nørskov, J. K. *Science* **2014**, *345*, 197–200.
- (13) Bader, R. F. W. *Atoms in Molecules: A Quantum Theory*; Oxford University Press: Oxford, 1994.
- (14) Bader, R. F. W. *J. Phys. Chem. A* **1998**, *102*, 7314–7323.
- (15) Keith, T. A. *AIMAll (Version 16.01.09, Aim.tkgristmill.com)*; TK Gristmill Software: Overland Park KS, USA, 2015.
- (16) Seeman, J. I. *J. Chem. Educ.* **1986**, *63*, 42.